Composites Science and Technology 157 (2018) 99–106

Contents lists available at ScienceDirect

Composites Science and Technology

journal homepage: http://www.elsevier.com/locate/compscitech

Failure mechanisms in bioinspired helicoidal laminates

J.L. Liu, H.P. Lee, V.B.C. Tan*

Department of Mechanical Engineering, National University of Singapore, 9 Engineering Drive 1, 117565, Singapore

ARTICLE INFO

Article history:
Received 25 September 2017
Received in revised form
2 January 2018
Accepted 20 January 2018
Available online 3 February 2018

Keywords:
Carbon fiber
Delamination
Mechanical properties
Finite element analysis
Biomimicry

ABSTRACT

Previous research has shown that stacking unidirectional laminates helicoidally with small interply angles resulted in improvements in transverse load resistance. Guided by computational simulations, damage evolution within helicoidal and cross-ply laminates was tracked with further experiments to offer an insight into key differences responsible for their distinct load bearing characteristics. Under transverse loads, the first form of damage is delamination. Unlike cross-plys, which suffer multiple delamination of about the same size throughout the thickness, delamination is harder to initiate in helicoidal laminates due to the small angle between each ply. A large delamination eventually formed at the mid-plane. Transverse cracks then appear on the tensile surface of both types of specimens and propagate upwards with increasing loads. Load drops occur whenever the transverse cracks propagate to the delamination immediately above them. In the case of cross-plys, where there are multiple delamination, multiple load drops occur. Load drops in helicoidal laminates are delayed until the cracks reach the large delamination in the mid-plane. Helicoidal specimens do not experience multiple loads drops and can attain high peak load before catastrophic failure. It is shown that even higher peak load is achieved by selectively seeding delamination in helicoidal laminates to further delay the merging of transverse cracks with the dominant delamination.

1. Introduction

Inspired by observations of the exoskeletal structure of crustaceans by Bouligand [1], stacking unidirectional carbon fiber composite helicoidally with small interply angles have shown great improvement in terms of maximum transverse load resistance as shown by Shang et al. [2], Apichattrabrut and Ravi-Chandar [3] and Cheng et al. [4]. Helicoidal configurations have unique load versus deformation curves that feature a very high stiffness towards the end with a single abrupt and catastrophic failure. A 34% increase in peak load for 19-ply helicoidal laminates over cross-ply ones was reported by Shang et al. [2]. The study by Hong and Liu [5], [15], as well as Lesser and Filippov [16] showed delamination area decreases as adjacent angle between plies decreases. This suggests the small ply angles of helicoidal configurations may make them more resistant to delamination. Andersons and König [6], Kim and Mayer [13] showed that decreasing the angle between plies will increase Mode II fracture toughness, which suggests the small angles in helicoidal configurations have greater Mode II fracture toughness. Ravi-Chandar [7] and Chen et al. [8], also performed experiments and simulations related to helicoidal laminates. The damage mechanisms of helicoidal configuration are compared with a common cross-ply configuration in this study to determine causes for their differences.

Although experiments and simulations have been carried out in previous studies, they focused primarily on the final damage of composites. Why helicoidal configurations outperform common cross-ply configurations is still not established. This study focuses on where cracks initiate, how damage grows and what causes final failure. Test specimens are subjected to different loadings to create cracks at different stages of loading. The damaged specimens are then sent for CT-scanning to examine the cracks to obtain a series of images showing how crack gradually grows until final failure. Computational simulation is also undertaken to obtain further insights.

2. Experimental and simulation procedures

2.1. Materials and stacking sequence

Cross-ply and helicoidal laminates were fabricated from unidirectional T700/2510 carbon-epoxy prepregs. The mechanical

* Corresponding author.
E-mail address: mpetanbc@nus.edu.sg (V.B.C. Tan).

https://doi.org/10.1016/j.compscitech.2018.01.033
0266-3538/

properties of the material have been previously reported [2]. Individual plies were cut into 100 × 100 mm squares and laid manually to form laminates of single helicoidal [0°/-10°/-20° …/-180°] and cross-ply [$(0°/90°)_9$/0°] configurations - denoted SH19 and CP19 respectively. They are cured in an oven under 30 kPa pressure. The temperature is raised from room temperature to 140 °C over 2 h and maintained for 2 h. The specimens are then cooled over 8 h to room temperature. Five specimens were initially produced for each configuration.

2.2. Transverse loading of specimens

Specimens were subjected to transverse point loads using the experimental set up and procedures described by Shang et al. [2]. The specimens are simply supported on one end of a circular cylinder with 75 mm internal diameter allowing the specimen to flex under transverse loading while providing out-of-plane constraint that is independent of in-plane orientation (Fig. 1). The load is applied at the center of the specimen at a rate of 1 mm/min using a 12 mm diameter hemispherical indenter.

Under transverse loading, cross-ply laminates showed multiple small load drops whereas helicoidal ones are characterized by a monotonically increasing load-displacement plot prior to a single catastrophic load drop [2]. In the tests reported here, specimens were not loaded to final failure. Instead, the tests are stopped at different points for different specimens. Micro-CT scans were then performed to track the damage evolution.

For CP19 samples, the first test was stopped at the first audible crack. Subsequent tests were stopped upon each load drop, as depicted in Fig. 2, to observe how cracks grew from one load drop to the next. As for SH19 samples, the first test was stopped at the first audible crack (specimen 1). The next test was until final load drop (specimen 5). This was followed by 3 other tests (specimens 2, 3 and 4), which were carried out to displacement intervals between specimens 1 and 5.

As the CT-scan system could accommodate specimens up to 30 mm wide only, the specimens were cut using water jet to fit into the machine. Each specimen was cut to a dimension of 30 × 100 mm centered at the point of loading. Six SH19 specimens were loaded until failure to ascertain specimen consistency. The maximum load was found to range from 5400 N to 5700 N. The specimen with a peak load of 5518 N was then selected as the reference specimen. The load-displacement plot of each new specimen was compared to this specimen. If there was a deviation of more than 5% in terms of load under same indenter displacement, that specimen would be disregarded and another specimen was prepared. Table 1 describes the corresponding stages of loading for each specimen.

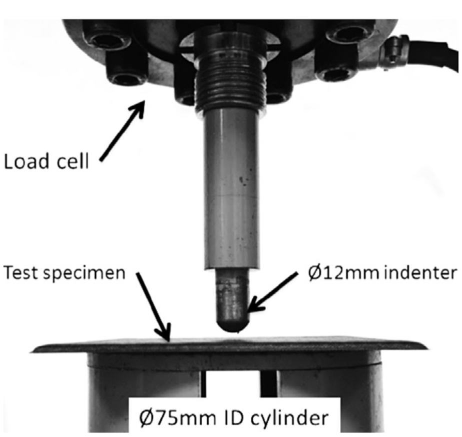

Fig. 1. Transverse loading experimental setup.

2.3. Numerical simulation of damage evolution

Finite element simulations replicating the experiments were performed using the parameters, model and methodology reported by Shang et al. [2]. The cohesive bond shear stiffness K_{ss} value of 2500 GPa/mm was adopted following the recommendation from Turon et al. [9]. The effects of delamination, fiber and matrix damage and their interactions were analyzed to determine where damage initiates, how damage evolves and what causes final failure.

Progressive failure analyses of cross-ply and helicoidal laminates under transverse point loading were performed. Maximum stress criterion was used for fiber-dominant failure, Tsai-Wu quadratic failure criterion for matrix-dominated failure [10] and mixed-mode decohesion elements for delamination [11]. Damage propagation in the simulation was handled through an energy based degradation model [12]. The model was constructed with 19 layers of 100 × 100 × 0.08 mm plies as shown in Fig. 3(a). Each ply consists of 8-node shell elements with reduced integration formulation (SC8R). Between every ply, a cohesive layer consisting of 3-D cohesive elements (COH3D8) is introduced to model interlaminar behavior. Ply damage in the simulation refers to matrix or fiber damage, damage in the cohesive layers represents delamination. Both ply and cohesive layers have similar mesh and the mesh is highly refined within a 20 × 20 mm area at the center of the laminate. The indenter is modeled as a 12 mm rigid hemisphere.

As shown in Fig. 3(b), delamination and fiber damage are captured at 4.5 mm indenter displacement, final load drop, and at 3 other intermediate displacements for SH19. For CP19, similar results are shown for 4.5 mm indenter displacement and at first load drop only. Elements became heavily distorted after that.

It should be noted that the simulations predict matrix damage occurring at very early stage of the loading. However, this does not lead to any significant load drops or change in stiffness. It is also difficult to detect matrix damage from CT scans in order to validate the simulations. As such, we have not included a conclusive analysis of the evolution of matrix damage.

3. Analysis of experimental and simulation results

3.1. Damage evolution in SH19

It is found from the simulations that at about 3 mm displacement, delamination initiates in cohesive layer 9 which, being located at the mid-plane, experiences the highest shear stress. The delamination continues to grow until final failure. Other cohesive layers also showed small areas of delamination but they remain limited in size until final failure. CT-scans also gave confirmation of one large delamination near the mid-plane of the laminate.

Fig. 4 shows the damage in the helicoidal laminate at the first audible crack. This occurred at a displacement of about 4.5 mm. At this displacement, simulations predict a 10 mm wide delamination forming at the mid-plane due to high transverse shear stresses. This is indicated by the state of finite elements in cohesive layer 9, which lies between plies 9 and 10. CT scans of the laminate also show a delamination at the mid-plane. It is difficult to measure the exact size of the delamination as it closes when the load is removed but it can be seen that the delamination is at least 5 mm wide.

At an indenter displacement of about 5 mm, Fig. 5 shows that the mid-plane delamination has grown slightly larger. This is evident in both CT-scans as well as FE simulations. Simulations also predict element failure due to fibre breakage in plies close to the